DAΦNE TECHNICAL NOTE

INFN - LNF, Accelerator Division

Frascati, July 22, 1997

Note: **MM-30**

FIELD QUALITY AND ALIGNMENT OF THE LARGE APERTURE QUADRUPOLES OF THE DAΦNE INTERACTION REGIONS

B. Bolli, F. Iungo, F. Losciale, M. Paris, M. Preger, C. Sanelli, F. Sardone, F. Sgamma, M. Troiani

1. Introduction

The 7 large aperture quadrupoles of the DAΦNE interaction regions have been delivered to LNF on April 23, 1997. The measurements on the prototype magnet are described in [1]. The field quality and the position of the magnetic and mechanical center have been measured for each magnet.

The measurements have been performed by the Magnetic Measurements Group with the DANFYSIK rotating coil system [2]. The integrated gradient, the average value of the field deviation from the quadrupole component at the boundary of the good field region (66 mm from the magnet axis) and the contribution of each individual high order component have been measured at 7 different excitation currents (≈ 100 A, ≈ 200 A, ≈ 300 A, ≈ 400 A, ≈ 460 A, ≈ 540 A, ≈ 590 A).

The position of the magnetic center has also been recorded with respect to the reference optical devices placed on top of the magnets. The mechanical center positions have been measured by the Alignment Group and the comparison between the results obtained by the two groups are described in Section 9. Here we anticipate that the vertical distance between the magnetic axis and the center of the alignment spheres has been found to be on average half a millimeter smaller than the distance between the mechanical axis and the sphere centers. The reason for this discrepancy was discovered after the completion of the measurements: the supports of the quadrupoles are made of soft iron, and part of the magnetic flux in the yoke, particularly when the magnet begins to saturate escapes through the support, thus creating an asymmetry between the upper and the lower part of the magnet.

Due to the tight schedule for the completion of the Main Rings assembly, it was decided to keep the iron support during the commissioning of the collider. Actually, these supports will not be used when DAΦNE will reach the operation regime, since the KLOE interaction region has only permanent magnet quadrupoles and special supports are being built for FI.NU.DA, which allow the large aperture quadrupoles to be rotated around the longitudinal axis in order to follow the prescriptions of the rotating frame method adopted to correct the coupling of the betatron oscillations due to the solenoidal fields of the detector.

The consequences of this choice on the alignment of the commissioning lattice are discussed in detail in Section 9. From the point of view of the field quality we remark that one quadrupole (Serial #7) has been completely characterized also without the iron support; the corresponding results are reported in the last row of each Table in the following as Serial #7ws (without support), but not taken into account for the calculation of the average and the r.m.s. deviation among the quadrupoles.

This Note contains all the measured values for the 8 quadrupoles, including the prototype (Serial #1). As already mentioned in [1], the working point for the FI.NU.DA. interaction region is in the linear region of the B-H curve of the quadrupoles, while the DAY-ONE structure and the D.E.A.R. one require two quadrupoles running in the linear region and the other two near saturation. The nominal good field region for these quadrupoles has been set at 66 mm, because the two beams cross them at a distance from the axis which depends on the crossing angle and on the lattice structure. However, following the procedure adopted for the other quadrupoles of the DAΦNE Main Rings, the analysis of the rotating coil output has been performed at a reference radius of 30 mm. For this reason, and also for a better comparison with the other magnets, the values of the overall field deviation are given at the reference radius of 30 mm. The contributions of the single high order components of the field are scaled at the nominal radius of 66 mm. They can be used to expand the field around the nominal trajectory in the magnets for beam tracking simulations.

Due to the small number of the magnets, it does not make much sense to show the distributions, as done previously in the case of the "small" [3] and "large" [4] quadrupoles. We give in each Table in the following the average value and the "rms" widths calculated as the average quadratic deviation.

2. Integrated gradient

The measurements have been performed by setting the power supplies always at the same nominal values, and the current detected by means of the precision DCCT system of the DANFYSIK system. However, a slight difference exists between the excitation currents of the series production magnets and those measured for the prototype. For this reason, the values obtained on the prototype have been properly scaled in order to normalize the distribution. We recall that each quadrupole has its own power supply and can therefore be calibrated individually. However, it is interesting to show how the integrated gradients are distributed around their average values.

Figure 1 shows the integrated gradient, averaged over the sample of the 8 magnets, as a function of the excitation current. Since the r.m.s. width of the distribution is too small to be seen in the figure, it is given in Table I, together with the measured values for each magnet at all excitation currents.

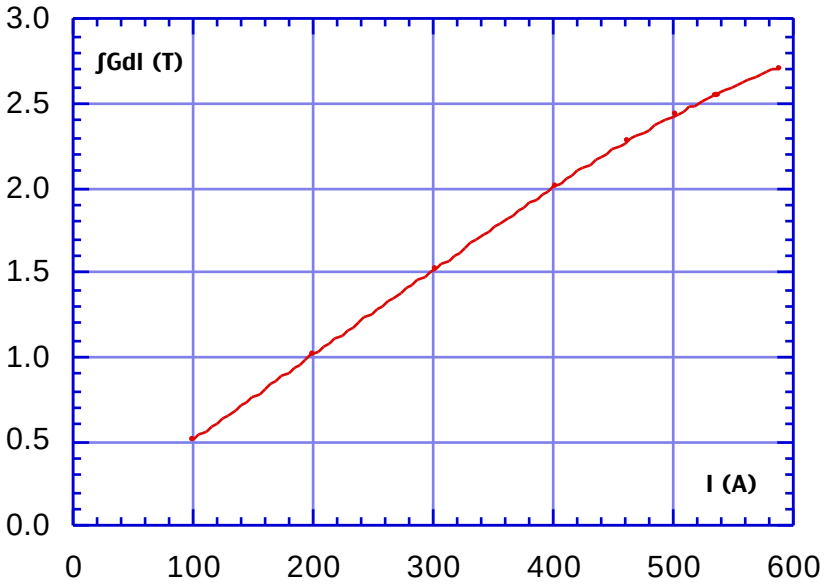

Fig. 1 - Average integrated gradient versus excitation current.

Table I - Integrated gradients

	100.52A	**200.91A**	**301.33A**	**401.77A**	**461.80A**	**502.16A**	**536.33A**	**587.46A**
#1	0.51043	1.01805	1.52258	2.01458	2.27821	2.43256	2.55042	2.71061
#2	0.50961	1.01683	1.52158	2.01369	2.27848	2.43383	2.55351	2.71294
#3	0.50917	1.01630	1.52093	2.01284	2.27689	2.43119	2.55182	2.71130
#4	0.50997	1.01793	1.52330	2.01657	2.28239	2.43825	2.55741	2.71715
#5	0.51038	1.01871	1.52450	2.01780	2.28360	2.43925	2.55873	2.71838
#6	0.50999	1.01772	1.52291	2.01618	2.28146	2.43699	2.55674	2.71657
#7	0.51012	1.01789	1.52317	2.01688	2.28203	-	2.55670	2.71631
#8	0.50965	1.01710	1.52191	2.01471	2.27928	2.43399	2.55306	2.71161
< >	**0.5099**	**1.0176**	**1.5226**	**2.0154**	**2.2803**	**2.4352**	**2.5548**	**2.7144**
rms	**0.0004**	**0.0008**	**0.0011**	**0.0017**	**0.0024**	**0.0030**	**0.0030**	**0.0031**
#7ws	0.51038	1.01908	1.52518	2.01924	2.28410	2.43882	2.55503	2.71253

3. Average deviation from the ideal field

As explained in Section 1, the data from the rotating coil system [2] have been analysed by setting the reference radius at 30 mm from the magnet axis. Of course it is possible to calculate the contribution of each harmonic component at the specified good field region radius of 66 mm, by multiplying the output of the code by the proper power of (66/30), but the single components must be added together with their phase in order to find the overall deviation from the ideal field at 66 mm.

The measurements on the prototype [1] have shown that the specified maximum deviation was exceeded, with the main contribution coming from the sextupole component. Since the main effect of this component is a slight change in the chromaticity of the ring, it is possible to correct it by means of the lumped sextupoles in the lattice, and therefore the magnet has been accepted. We show in Table II the overall deviation from the ideal quadrupole field at 30 mm from the magnet axis for all the magnets at all measured currents. Its average and standard deviation are also shown in Fig. 2.

Table II - Relative deviation from the ideal quadrupole field @ 30 mm (units of 10^{-4})

	100.52A	**200.91A**	**301.33A**	**401.77A**	**461.80A**	**502.16A**	**536.33A**	**587.46A**
#1	1.166	1.287	1.419	1.725	2.468	3.733	5.338	8.512
#2	1.871	1.421	1.586	1.903	2.471	3.870	5.963	9.137
#3	2.973	2.709	2.705	3.138	3.755	5.007	7.099	10.310
#4	1.138	1.221	1.547	2.126	2.627	3.802	5.646	8.731
#5	1.429	1.056	1.153	1.853	2.802	4.301	6.034	9.072
#6	2.422	2.224	1.880	1.985	2.526	3.886	5.848	9.156
#7	2.379	2.048	1.843	1.855	2.473	-	5.542	8.543
#8	1.525	0.948	1.164	1.591	2.076	3.315	5.144	8.402
< >	**1.863**	**1.614**	**1.662**	**2.022**	**2.650**	**3.988**	**5.825**	**8.983**
rms	**0.668**	**0.634**	**0.500**	**0.478**	**0.491**	**0.534**	**0.597**	**0.614**
#7ws	1.822	1.648	1.521	1.475	1.680	1.935	2.582	3.343

As can be noticed from the last row in Table II**, the field quality improves significantly <u>when the iron support is removed</u>. Scaling the overall deviation at the specified good field region of 66 mm (at the nominal current of 460 A) and taking into account the measurement errors, the magnet meets the specified field quality.**

The conclusions drawn in [1] are therefore valid only for the magnet placed on the soft iron support, **while the quadrupole alone is within Specification.**

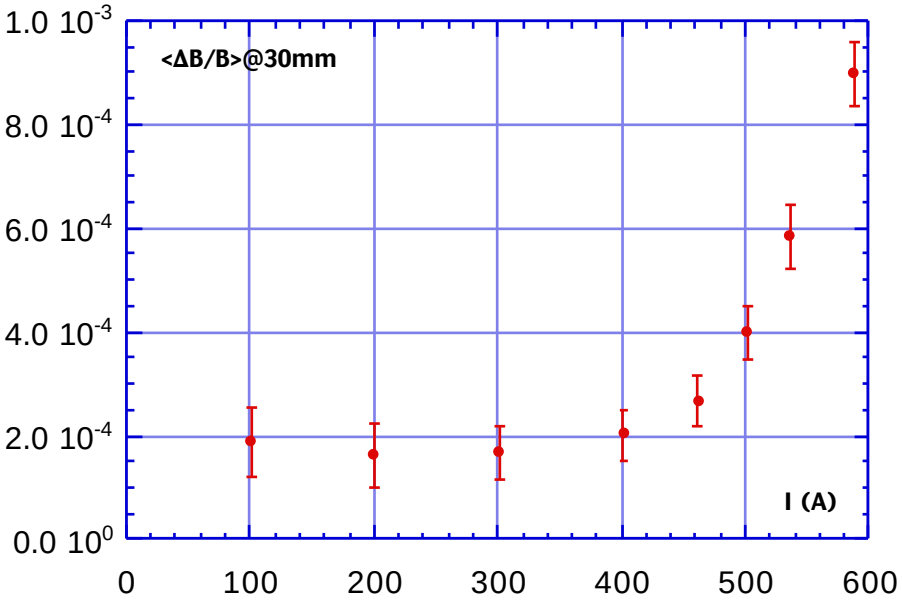

Figure 2 - Average relative deviation from the ideal quadrupole field @ 30 mm. Error bars are the r.m.s. deviations of the distributions.

4. Sextupole term

The contribution of the sextupole term to the overall deviation from the ideal field at 66 mm from the axis is given in Table III, and its value averaged over the sample of 8 magnets plotted versus the excitation current in Fig. 3. The phase of the sextupole component is randomly distributed between 30° and 160°. Comparing Fig. 3 to Fig. 2 and scaling the values by the ratio of the two different radii (66/30) it appears clearly that the sextupole term accounts for most of the deviation from the ideal field at high current. Comparing with Table II it is clear that the improvement of the field quality at high current when the iron support is removed comes mainly from the corresponding improvement in the sextupole term.

Table III - Sextupole contribution divided by the ideal quadrupole field on a circle of 66 mm radius around the magnet axis (units of 10^{-4})

	100.52A	**200.91A**	**301.33A**	**401.77A**	**461.80A**	**502.16A**	**536.33A**	**587.46A**
#1	2.508	2.776	3.060	3.758	5.403	8.191	11.728	18.713
#2	4.110	3.120	3.483	4.184	5.430	8.512	13.119	20.101
#3	6.523	5.944	5.938	6.893	8.248	11.000	15.613	22.682
#4	2.405	2.644	3.379	4.649	5.766	8.358	12.412	19.202
#5	3.095	2.297	2.486	4.046	6.134	9.449	13.262	19.952
#6	5.306	4.888	4.134	4.363	5.553	8.549	12.866	20.143
#7	5.163	4.440	3.995	4.057	5.412		12.170	18.784
#8	3.318	1.934	2.523	3.491	4.558	7.289	11.312	18.482
< >	**4.053**	**3.505**	**3.625**	**4.430**	**5.813**	**8.764**	**12.810**	**19.757**
rms	**1.487**	**1.418**	**1.112**	**1.055**	**1.079**	**1.173**	**1.317**	**1.354**
#7ws	3.925	3.571	3.298	3.205	3.659	4.226	5.610	7.291

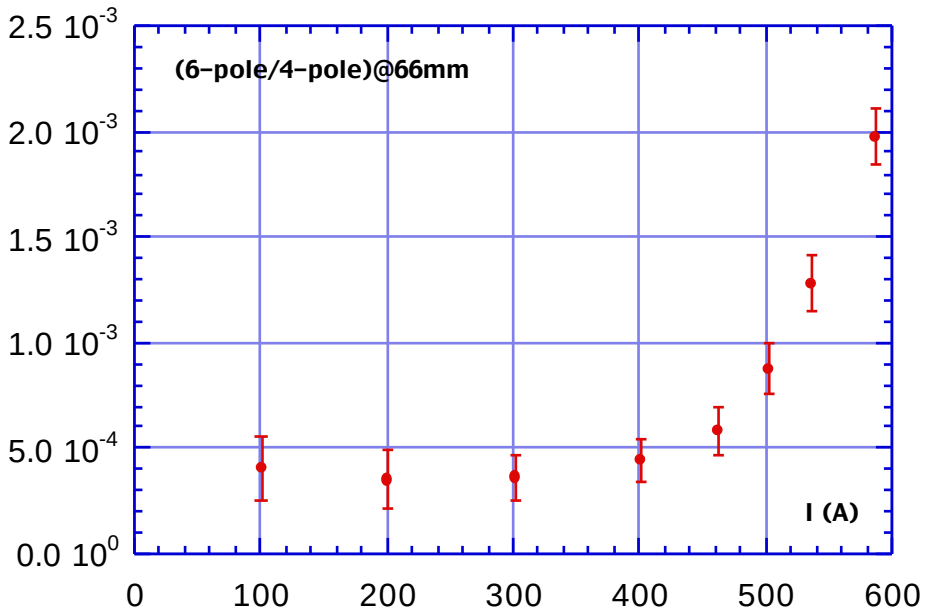

Figure 3 - Sextupole/quadrupole @ 66 mm averaged over the 8 quads
(error bars are the r.m.s. deviations of the distributions)

5. Octupole term

The contribution of the octupole term to the overall deviation is given in Table IV and Fig. 4, where the scale is much more expanded than in Fig. 3. The phase is distributed at random. The effect of the iron support is negligible.

Table IV - Octupole contribution divided by the ideal quadrupole field
on a circle of 66 mm radius around the magnet axis (units of 10^{-4})

	100.52A	**200.91A**	**301.33A**	**401.77A**	**461.80A**	**502.16A**	**536.33A**	**587.46A**
#1	1.593	1.672	1.808	1.640	1.519	1.697	1.549	1.885
#2	0.718	0.628	0.567	0.331	0.702	0.314	0.201	0.492
#3	1.473	1.365	1.225	1.176	1.346	1.868	1.229	1.342
#4	2.018	1.476	1.345	1.692	1.268	1.034	1.535	1.727
#5	1.447	0.940	1.488	1.453	1.618	1.191	1.352	1.101
#6	1.597	0.890	0.561	0.610	0.428	0.328	0.494	0.677
#7	2.561	2.327	2.004	1.376	1.692	-	2.400	2.496
#8	1.566	2.007	1.342	0.793	1.018	0.871	1.225	1.519
< >	**1.622**	**1.413**	**1.293**	**1.134**	**1.199**	**1.043**	**1.248**	**1.405**
rms	**0.523**	**0.582**	**0.518**	**0.502**	**0.450**	**0.606**	**0.674**	**0.654**
#7ws	2.379	1.929	1.819	1.536	1.544	1.545	2.666	2.942

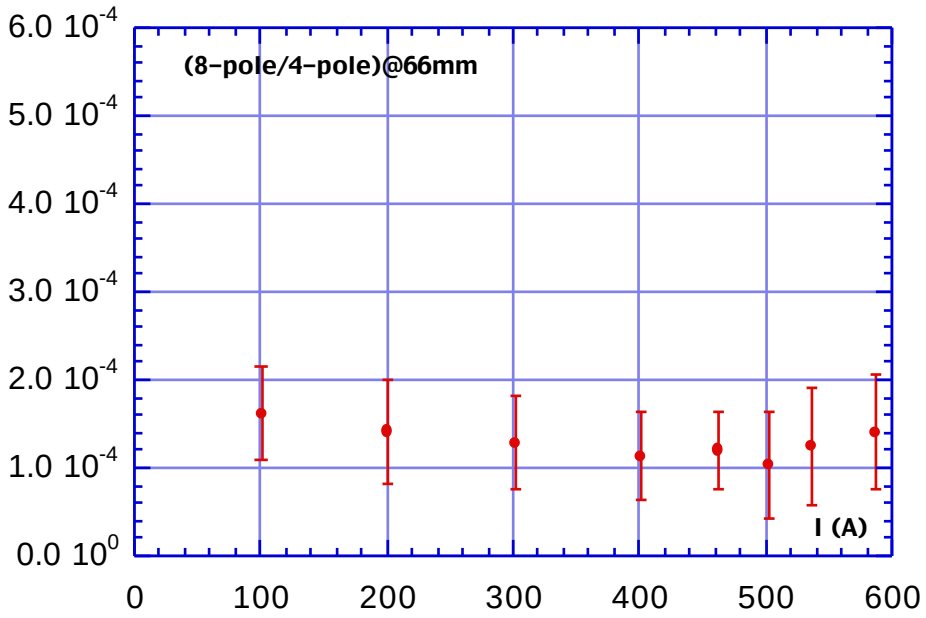

Figure 4 - Octupole/quadrupole @ 66 mm averaged over the 8 quads
(error bars are the r.m.s. deviations of the distributions)

6. Decapole term

The contribution of the 10-pole term to the overall deviation is given in Table V and Fig. 5: the scale is the same as in Fig. 4. The phase is distributed at random. The contribution of the decapole term is becomes slightly smaller when the iron support is removed.

Table V - Decapole contribution divided by the ideal quadrupole field
on a circle of 66 mm radius around the magnet axis (units of 10^{-4})

	100.52A	**200.91A**	**301.33A**	**401.77A**	**461.80A**	**502.16A**	**536.33A**	**587.46A**
#1	0.365	0.306	0.681	0.172	0.145	0.477	0.589	0.442
#2	1.131	0.151	0.221	0.659	0.283	0.220	0.627	1.311
#3	1.637	1.415	1.348	1.031	1.228	1.873	1.802	1.724
#4	1.218	0.577	0.385	1.116	0.868	0.363	0.773	1.312
#5	1.132	0.670	0.718	0.215	1.165	1.231	0.763	0.644
#6	1.282	0.408	0.211	0.349	0.086	0.227	1.037	0.777
#7	1.638	1.412	1.544	1.194	1.439	-	2.115	2.436
#8	0.965	1.654	0.671	0.569	0.508	0.660	1.450	1.673
< >	**1.171**	**0.824**	**0.722**	**0.663**	**0.715**	**0.721**	**1.144**	**1.290**
rms	**0.404**	**0.581**	**0.492**	**0.409**	**0.529**	**0.616**	**0.578**	**0.660**
#7ws	1,381	0.913	0.324	0.845	0.783	0.908	1.768	2.016

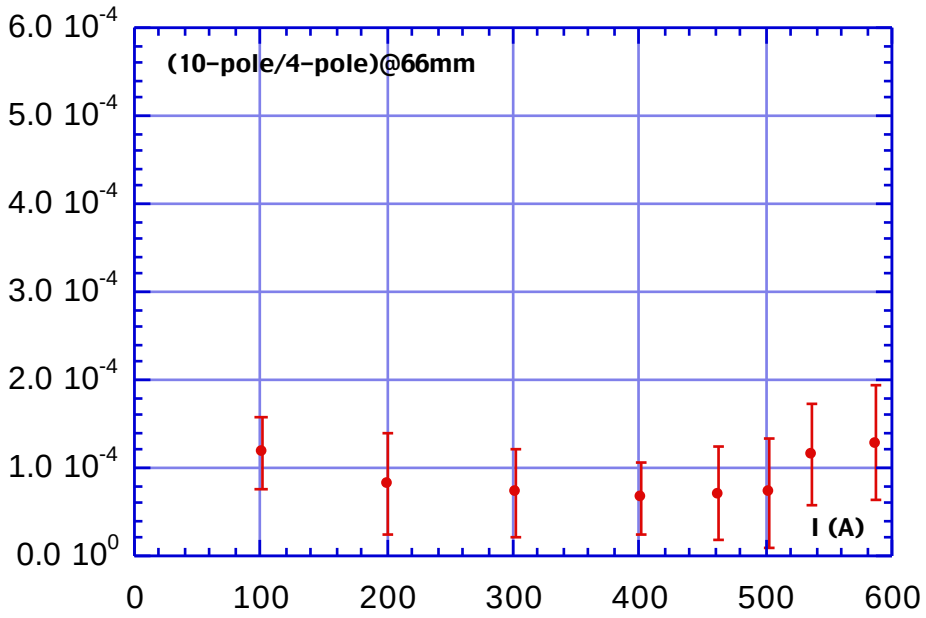

Figure 5 - Decapole/quadrupole @ 66 mm averaged over the 8 quads
(error bars are the r.m.s. deviations of the distributions)

7. Twelve-pole term

The 12-pole is the first systematic high order component with the same symmetry of the main quadrupole term. Its contribution to the overall deviation from the ideal field has been minimised by chamfering the end caps of the poles in the prototype magnet [1], optimizing the correction at the excitation current of 300 A.

The residual contribution in the whole operating range is shown in Fig. 6, and the values for all the magnets given in Table VI. The phase of the 12-pole harmonic is typically opposite to the main quadrupole one. However, after reducing its contribution to a very small amount with the chamfering procedure, the measured values of the phase tend to be spread around π ($150° \lessapprox \varphi \lessapprox 240°$). The presence of the iron support does not change substantially the amount of the 12-pole harmonic.

Table VI - 12-pole contribution divided by the ideal quadrupole field
on a circle of 66 mm radius around the magnet axis (units of 10^{-4})

	100.52A	**200.91A**	**301.33A**	**401.77A**	**461.80A**	**502.16A**	**536.33A**	**587.46A**
#1	1.466	0.935	0.831	1.327	2.598	3.008	3.329	4.228
#2	1.317	1.295	1.030	1.408	2.251	2.283	2.633	3.622
#3	1.086	1.250	0.837	1.485	2.013	2.174	2.879	3.718
#4	1.650	0.943	0.974	0.635	1.591	2.357	2.490	3.448
#5	0.857	0.982	0.349	1.173	2.205	3.586	3.465	3.575
#6	1.015	0.625	0.454	1.108	1.837	1.848	2.085	3.247
#7	1.100	0.731	1.130	0.688	1.464	-	2.511	2.699
#8	1.397	2.511	1.311	1.304	1.691	1.933	3.038	2.987
< >	**1.236**	**1.159**	**0.864**	**1.141**	**1.956**	**2.455**	**2.804**	**3.440**
rms	**0.265**	**0.592**	**0.326**	**0.319**	**0.382**	**0.625**	**0.463**	**0.469**
#7ws	1.647	0.895	0.613	1.339	1.667	2.178	2.361	3.022

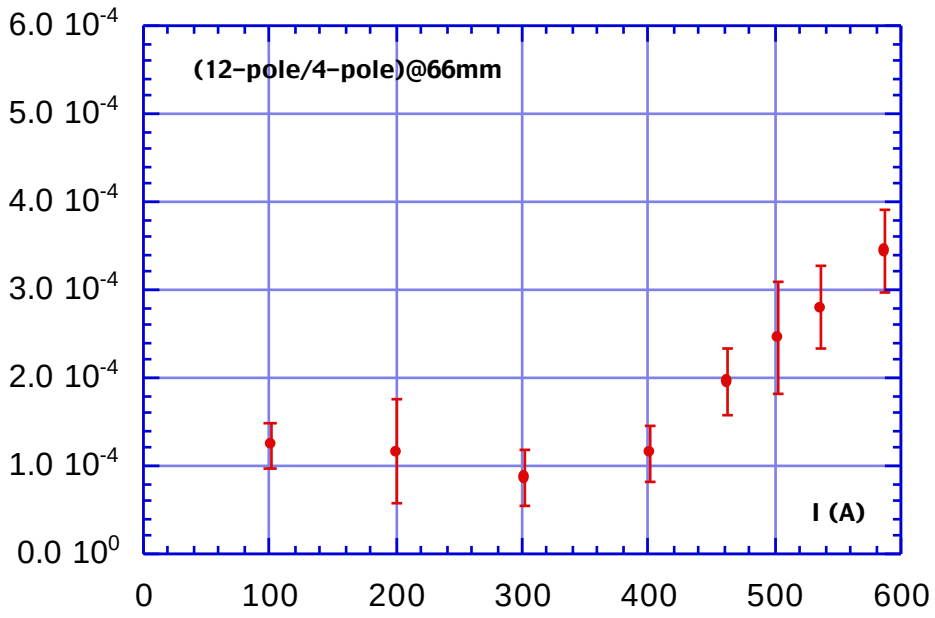

Figure 6 - 12-pole/quadrupole @ 66 mm averaged over the 8 quads
(error bars are the r.m.s. deviations of the distributions)

8. Twenty-pole term

As well as the 12-pole term, also the 20-pole is a systematic high order harmonic with the same symmetry of the main quadrupole component. Figure 7 shows the 20-pole component, averaged over the sample of the 8 magnets as a function of the excitation current. For the large aperture quadrupoles its contribution is rather small at the radius of the rotating coil (49 mm), at the limit of the sensitivity of the measuring system, and this clearly appears from the results displayed in the figure, where the widths of the distribution are of the same order of the average values. The relative weight at the good field region boundary is however rather large, since the measured contributions are multiplied by $(66/49)^8=10.8$. The values for the single magnets are given in Table VII. The iron support does not affect, within the measurement uncertainty, the contribution of the 20-pole term.

Table VII - 20-pole contribution divided by the ideal quadrupole field on a circle of 66 mm radius around the magnet axis (units of 10^{-4})

	100.52A	**200.91A**	**301.33A**	**401.77A**	**461.80A**	**502.16A**	**536.33A**	**587.46A**
#1	4.287	2.777	1.470	1.100	5.478	4.049	2.522	2.592
#2	5.480	3.055	3.228	2.475	2.468	3.329	3.278	2.383
#3	4.550	3.898	2.464	5.108	2.861	5.987	2.866	2.818
#4	7.672	4.014	1.816	3.602	0.841	2.478	1.442	1.270
#5	7.298	3.656	3.250	0.725	13.840	5.729	6.958	2.191
#6	6.097	3.071	2.289	0.735	3.726	3.142	3.183	0.279
#7	4.608	5.526	5.404	2.332	4.194	-	6.003	4.355
#8	3.113	8.045	4.916	2.976	6.097	3.199	4.002	4.336
< >	**5.388**	**4.255**	**3.105**	**2.382**	**4.938**	**3.988**	**3.782**	**2.528**
rms	**1.562**	**1.755**	**1.415**	**1.530**	**3.966**	**1.359**	**1.836**	**1.387**
#7ws	4.939	2.785	1.281	4.520	4.494	3.130	5.367	6.410

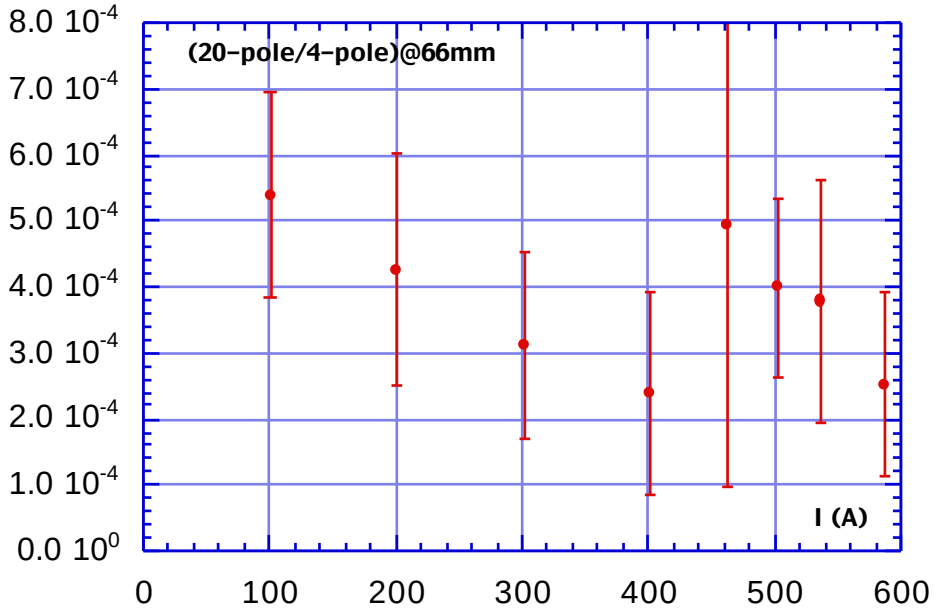

Figure 7 - 20-pole/quadrupole @ 66 mm averaged over the 8 quads
(error bars are the r.m.s. deviations of the distributions)

9. Alignment

As mentioned in Section 1, the positions of the magnetic and mechanical centers of all the quadrupoles were measured independently before discovering the problem of the iron support. We present here the results of these preliminary measurements, obtained by following the procedure adopted for the large quadrupoles of the Main Rings achromats. For sake of simplicity we show the results for all magnets together, indicating if they are of the "right" or "left" type (according to which side the electric connections and hydraulic fittings come out) by setting an "R" or an "L" after the serial number. Table VIII shows the results obtained for the magnetic centers at the excitation current of 536.34A. The values of the rotation of the magnetic horizontal symmetry plane with respect to the mechanical ones are those directly given by measuring system, without correction for recalibration [5] and irrespective of the "right" or "left" type of the quadrupole. Table IX shows the corresponding values for the mechanical centers. Table X summarizes the results on the distance between the magnetic and mechanical center positions, the tilts between the longitudinal axis position during the magnetic measurements and the mechanical ones and the rotation of the horizontal symmetry plane after correction for recalibration [5]. Figure 8 is the X-Y plot of the shifts.

Table VIII - Magnetic center position of the large aperture quadrupoles (I = 536.34 A)

Serial #	XAmag	XBmag	YAmag	YBmag	Φ(mrad)
#1R	13.30	14.65	499.99	499.92	0.96
#2R	13.14	15.09	499.90	499.84	1.19
#3L	14.04	14.06	499.81	499.78	0.39
#4L	13.89	13.78	499.89	499.86	0.19
#5L	14.46	14.38	499.86	499.84	-0.00
#6R	13.61	14.73	499.89	499.82	0.98
#7R	13.72	14.39	499.75	499.68	0.28
#8L	14.32	14.47	499.81	499.77	-0.22

Table IX - Mechanical center position of the large aperture quadrupoles (I = 536.34 A)

Serial #	XAmec	XBmec	YAmec	YBmec
#1R	12.88	13.19	500.23	500.28
#2R	13.08	13.53	500.40	500.35
#3L	12.90	13.35	500.44	500.41
#4L	13.26	13.21	500.46	500.36
#5L	13.28	13.11	500.44	500.31
#6R	13.11	13.46	500.27	500.27
#7R	12.89	13.36	500.33	500.32
#8L	13.24	13.44	500.25	500.29

Table X - Distance (mm) and tilt (mrad) between the magnetic and mechanical axis

Serial#	Shift X	Shift Y	Tilt X	Tilt Y	Shift XC	Φ(mrad)
#1R	0.52	-0.30	-12.53	0.80	0.04	0.26
#2R	0.75	-0.51	-10.77	0.07	0.16	0.49
#3L	0.22	-0.63	12.33	0.00	0.02	-0.31
#4L	0.03	-0.53	8.03	-0.47	-0.07	-0.51
#5L	-0.05	-0.53	16.33	-0.73	-0.05	-0.70
#6R	0.38	-0.41	-11.77	0.47	-0.11	0.28
#7R	0.10	-0.61	-12.40	0.40	-0.04	-0.42
#8L	0.02	-0.48	14.07	0.53	0.13	-0.92

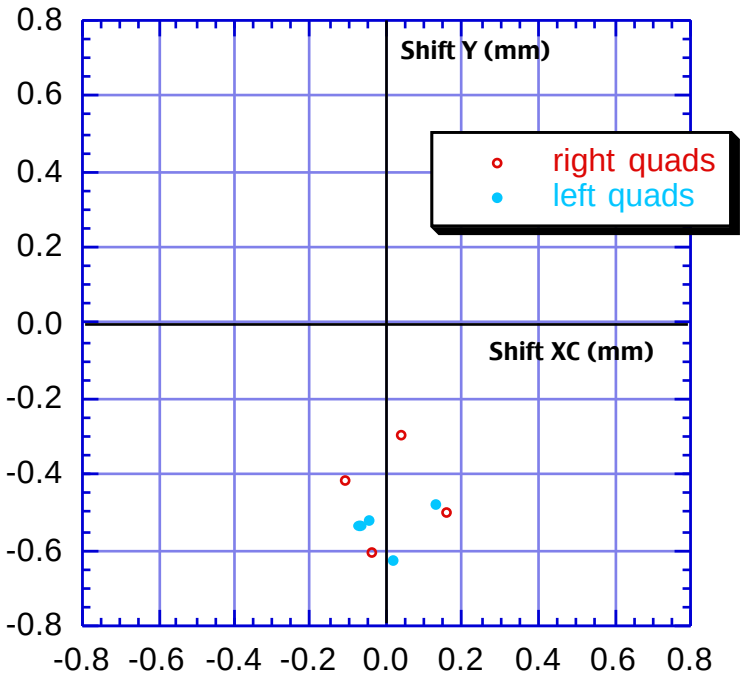

Figure 8 - Distance between magnetic and mechanical axes of the large aperture quadrupoles.

As clearly shown in Fig. 8, there is an average vertical asymmetry in the quadrupoles of ≈0.5 mm, due to the iron support. Since the asymmetry could depend on the degree of saturation in the magnet, we measured the variation of the magnetic center position as a function of the excitation current in quadrupole Serial #7. The support was then substituted with a provisional one obtained by means of wood blocks and the measurement of the vertical distance between the magnetic and mechanical center repeated at all excitation currents.

As shown in Fig. 9, the distance between the magnetic and mechanical centers at 534 A was reduced from -0.65 mm to -0.30 mm when the iron support was removed. If the same reduction of 0.35 mm is applied to all the numbers in the ShiftY column in Table X, the average distance drops to -0.15 mm. Moreover, Fig. 9 shows that also without the iron support the distance between the magnetic and mechanical axes increases at high current, and this saturation effect is explained by a residual magnetic asymmetry in the quadrupole, due to the fact that the lower iron plates welded on the laminations are larger than the upper ones. Extrapolating the behaviour in Fig. 9 to all the 8 quadrupoles and considering only the measurements taken below 400 A without the iron support, we find an average distance between the magnetic and mechanical centers of only 0.05 mm.

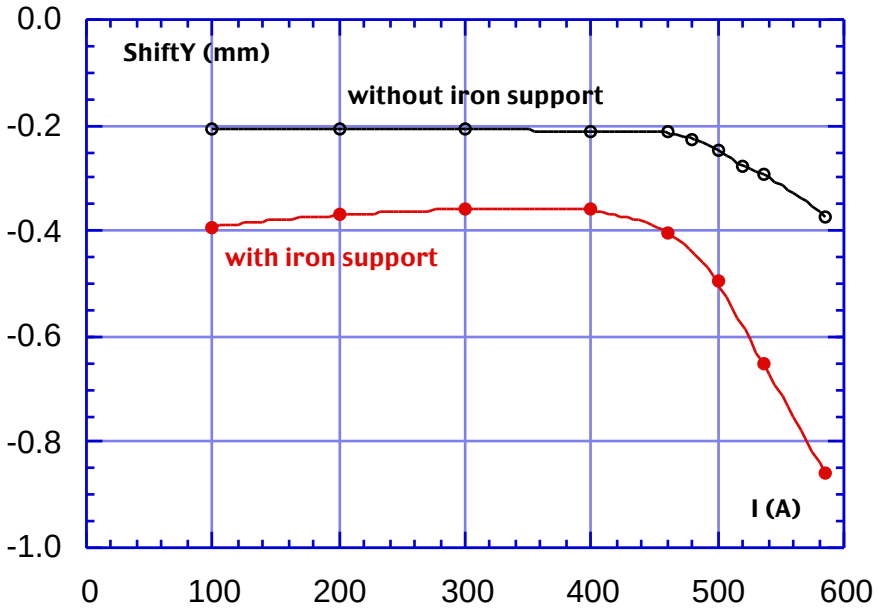

Figure 9 - Vertical distance between magnetic and mechanical center of Quadrupole #7 versus excitation current

In order to check that the dependence of the distance between the magnetic and mechanical center behaves in the same way for all the quadrupoles, we performed the same measurement on other 3 quadrupoles (Serial #2, #3 and #5). The result, including #7, is shown in Fig. 10, where the four curves are normalized to zero at the nominal current of 534 A, in order to be easily compared. They are quite similar, and it is therefore reasonable, within the overall alignment tolerance, to take their average values to correct the position of the vertical magnetic center as a function of the operating current.

Table XI gives these average values together with the r.m.s. dispersion over the four measured magnets.

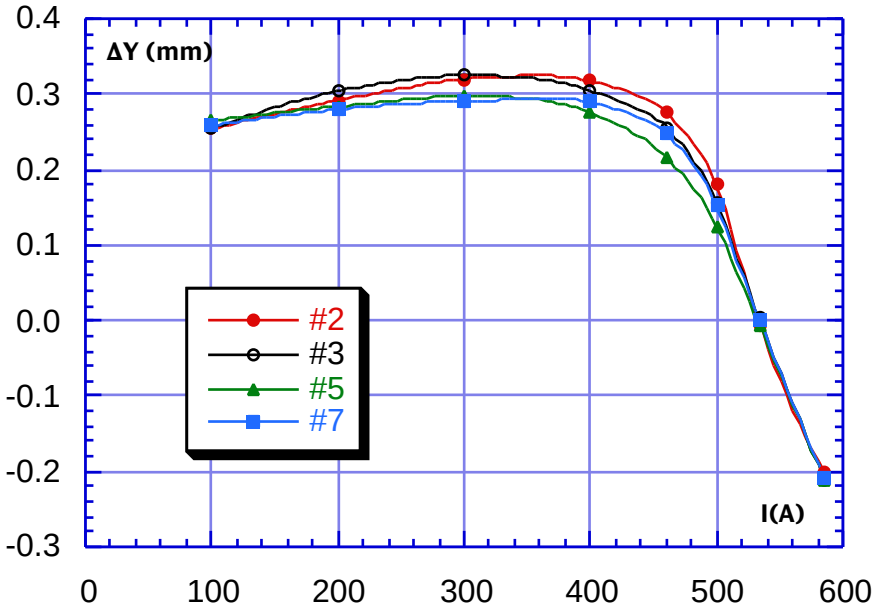

Figure 10 - Shift of the measured vertical position of the magnetic center versus current. (All curves normalized at 534 A).

Table XI - Correction of the vertical magnetic center position (ΔY) versus current

I(A)	ΔY (mm)	r.m.s.
100	0.258	0.005
200	0.290	0.011
300	0.309	0.016
400	0.297	0.018
460	0.250	0.025
500	0.155	0.023
534	0.000	0.000
585	-0.208	0.004

Starting from the lattice constants of the interaction region [6], we can now set the alignment positions for the large aperture quadrupoles. Table XII indicates the required integrated gradients, currents and interpolated vertical corrections for the corresponding quadrupoles (the serial numbers are indicated within parentheses in the first column).

Table XII - Integrated gradient, current and vertical correction

Lattice	∫Gdy (T)	I(A)	ΔY (mm)
DAY-ONE (#1,#4,#6.#8)	2.55	531	0.01
DAY-ONE (#2,#3,#5,#7)	1.39	274	0.31
D.E.A.R. (#1,#4)	2.79	>600	-0.21
D.E.A.R. (#2,#5)	1.26	249	0.30
FI.NU.DA. (#1,#4)	1.27	252	-
FI.NU.DA. (#2.#5)	0.84	168	-

The required gradient for quadrupoles #1 and #4 in the D.E.A.R. lattice is larger than the maximum allowed and should be decreased. The correction in Table XII corresponds to the maximum current (585 A). The correction factor for FI.NU.DA. is not indicated, since the quadrupoles will be placed on a special rotating support, and the position of the magnetic center will be measured again in the final configuration.

As shown in Table X, the absolute values of the azimuthal rotation of the horizontal symmetry plane for all the quadrupoles exceed the threshold of 0.25 mrad assumed to align the magnets without rotation. In order to indicate the numbers for the final alignment of the magnets in the interaction regions, we can therefore apply for the horizontal positioning the formulas given at paragraph 6b) in [5]. The heights of the Taylor-Hobson sphere centers must however be corrected by the values of ΔY given in Table XII, namely

$$\text{HeightA} = \text{YAmec} + \text{ShiftY} + \Delta Y$$
$$\text{HeightB} = \text{YBmec} + \text{ShiftY} + \Delta Y$$

Table XIII gives the indications for the alignment of the large aperture quadrupoles on the DAY-ONE lattice. The magnets, seen from the electrical and cooling connection side, must be rotated counterclockwise when the sign of Φ is positive. Table XIV shows the variations in the vertical position required for the D.E.A.R. structure, due to the different excitation currents: the quadrupoles in the first four rows are those surrounding the D.E.A.R. detector, while the last four are those on the other side (the KLOE interaction region). The latter must be changed only if the central quadrupole is removed also on this side to make the collider more symmetric. From the comparison of the two tables it is clear that only the quadrupole pairs nearest to the interaction point must be corrected.

Table XIII - Alignment data for the DAY-ONE lattice

Serial#	Slit A	Slit B	Height A	Height B	Φ(mrad)
#1R	12.71	13.36	499.94	499.99	0.26
#2R	12.68	13.93	500.20	500.15	0.49
#3L	12.77	13.48	500.12	500.09	0.31
#4L	12.94	13.53	499.94	499.84	0.51
#5L	12.88	13.51	500.22	500.09	0.70
#6R	13.08	13.49	499.87	499.87	0.28
#7R	13.14	13.11	500.03	500.02	-0.42
#8L	12.91	13.77	499.78	499.82	0.92

Table XIV - Vertical positioning of the quadrupoles for the D.E.A.R. lattice

Serial#	Height A	Height B
#1R	499.72	499.77
#2R	500.19	500.14
#4L	499.72	499.62
#5L	500.21	500.08
#3L	500.11	500.08
#6R	499.65	499.65
#7R	500.02	500.01
#8L	499.56	499.60

The data for FI.NU.DA. will be available after the magnetic center position measurement with the final support.

8. Conclusions

The field quality of the large aperture quadrupole, measured without the iron support, is significantly better than the result given in the Technical Note describing the measurements on the prototype [1] and the magnet meets the field quality Specification. Since the large aperture quadrupoles will be used in the final configuration of DAΦNE only on the FI.NU.DA. interaction region, and they will have a completely different, iron free, rotating support, the sextupole contribution at high current is expected to be smaller.

The vertical position of the magnetic center with the final support should be measured again.

For the D.E.A.R. structure the required integrated gradient of the inner couple of quadrupoles exceeds the maximum allowed excitation current. The lattice must be modified accordingly.

References

[1] B. Bolli, F. Iungo, N. Ganlin, F. Losciale, M. Paris, M. Preger, C. Sanelli, F. Sardone, F. Sgamma, M. Troiani: "The large aperture quadrupole prototype for the DAΦNE interaction regions" - DAΦNE Technical Note MM-22 (27/1/1996).

[2] F. Iungo, M. Modena, Q. Qiao, C. Sanelli: "DAΦNE Magnetic Measurements Systems" - DAΦNE Technical Note MM-1 (4/11/1993).

[3] B. Bolli, N. Ganlin, F. Iungo, F. Losciale, M. Preger, C. Sanelli, F. Sardone: "Field quality of the small quadrupoles for the DAΦNE Main Rings" - DAΦNE Technical Note MM-10 (22/2/1996).

[4] B. Bolli, N. Ganlin, F. Iungo, F. Losciale, M. Preger, C. Sanelli, F. Sardone: "Field quality of the large quadrupoles for the DAΦNE Main Rings" - DAΦNE Technical Note MM-24 (22/4/1997).

[5] B. Bolli, N. Ganlin, F. Iungo, F. Losciale, M. Paris, M. Preger, C. Sanelli, F. Sardone, F. Sgamma, M. Troiani: "Comparison of magnetic and mechanical center positions of the large quadrupoles and sextupoles in the DAΦNE Main Rings" - DAΦNE Technical Note MM-27 (23/5/1997).

[6] M.E. Biagini, C. Biscari, S. Guiducci: "DAΦNE Main Rings Lattice Update" - DAΦNE Technical Note L-22 (18/3/1996).